Active and Passive Camber Morphing for Helicopter Rotors towards Performance Improvements in Hover and Vertical Flight

Kushagra Vidyarthi
Researcher

Yasir Zahoor
PhD Student

Marilena D Pavel
Associate Professor

Roeland De Breuker
Associate Professor

Faculty of Aerospace Engineering
Delft University of Technology
Delft, The Netherlands

Mark Voskuijl
Professor
Faculty of Military Sciences,
Netherlands Defence Academy
Den Helder, The Netherlands

ABSTRACT

Rotor morphing has been investigated in the past for improvement of rotor performance, either for reduction of rotor power demand or for vibratory load alleviation. The present study investigates the application of camber morphing for improvement of rotor performance in hover and vertical flight conditions, with a particular focus on the combination of camber morphing systems and variable RPM rotors. Camber morphing utilizes a smooth flap at the trailing edge of the rotor blade to modify the camber of blade airfoil sections without excessive drag penalties. Two different camber morphing systems will be investigated in this study, namely the active and passive systems. Passive camber morphing, which combines camber morphing with the variable speed rotor concept is the unique aspect of camber morphing which will be the primary focus of this study. The active system can be actuated at frequencies higher than 1/rev of the rotor and requires external power input for functioning. The passive system can be controlled only by varying the RPM of the rotor and requires no additional energy input. Therefore, the passive system is expected to show larger net performance benefits. Variable RPM rotors in themselves show potential towards the reduction of rotor power demand but are largely ineffective for low-speed applications. The combination of camber morphing and the variable speed rotor shows larger performance benefits than those obtained from the two technologies independent of each other. The two technologies, when combined in passive camber morphing, can remedy each other's deficiencies and improve the overall rotor performance. The use of camber morphing shows more benefit for operating points at or near the edge of the flight envelope since the rotor blade sections encounter high average angles of attack for these operating points. Vertical climb and hover at high altitude are examples of flight conditions investigated. Overall, passive camber morphing shows a larger performance benefit as compared to the active system.

INTRODUCTION

From the very first helicopters, the main rotor system of the vehicle has been designed by taking into account the different flight conditions the vehicle will encounter. This means that the main rotor is a multi-point design, which operates at sub-optimal or near-optimal efficiency in all flight conditions. The performance of the rotor directly influences the overall fuel consumption and emissions of the helicopter, and any inefficiencies in the system will negatively impact these parameters. Therefore, with increasingly strict environmental norms being imposed on the aviation industry, it has become necessary to address these apparent inefficiencies of the main rotor system of the helicopter.

Many different methods have been considered in the past for rotor performance improvement and vibratory load reduction (Ref. 1). These include Higher Harmonic Control (HHC) as well as On-Blade Control (OBC) devices. Rotor morphing typically falls under OBC methods and has been considered in the past as a means to improve the performance of the rotor. With the advent of tailorable materials and advanced manufacturing techniques, it has become possible to develop structures that can adapt their shape in response to different flight conditions encountered by a helicopter.

Various studies have investigated different categories of morphing systems in the past, primarily as a means to supplement the performance of a predefined rotor geometry.

Presented at the VFS 76th Annual Forum & Technology Display, October 6–8, 2020, Virtual.

Kerho (Ref. 2) has investigated variable leading edge droops to alleviate dynamic stall on the retreating blade. Khoshaljeh et al. (Ref. 3) have investigated chord extension systems in the form of trailing edge plates aimed at modifying local aerodynamic coefficients of blade sections, with a power reduction of 9% - 15% obtained in this study depending on the flight condition. The authors have also indicated that rotor morphing is useful primarily at the edge of the flight envelope, e.g.- at high advance ratios, or for high altitude operations. The integration of these devices with the rotor has been explored by Gandhi and Hayden (Ref. 4).

Friedmann has summarized the recent developments related to on-blade control (OBC) for vibration and noise reduction in his work (Ref. 1). The author has described the application of actively controlled trailing edge flaps (TEFs), active twist methods, and gurney flaps for these applications, and has provided a comparison of these devices with higher harmonic control (HHC) methods. It is stated that the OBC devices perform better than HHC methods in terms of actuation power demand, system bandwidth, and location on the rotor blade. OBC devices also allow individual inputs to be provided to each blade, which is not possible with HHC. Friedmann has described two distinct phenomena through which active TEFs affect rotor performance. These are the direct lift effect and the servo flap effect. Through the direct lift effect, the flap generates additional lift which is used to modify vibration and noise characteristics of the blade. The servo flap effect is responsible for a change in the angle of attack of the blade section, which results in a modification of the blade loading. In his review, Friedmann (Ref. 1) has found that the most effective location for the TEF is around 75% blade span with a flap span of 12% and flap chord equal to 25% of local airfoil chord.

Koratkar and Chopra have also investigated the application of trailing edge flaps actuated by piezoelectric benders for vibration control in their work (Ref. 5) (Ref. 6). The authors state that the piezoelectric benders used for actuation are lightweight and compact, and will allow for multiple spanwise flaps to be placed on the same blade. During the experimental verification of the concept using a Froude-scaled rotor model (Ref. 5), the authors found that the maximum deflection of the TEF is heavily influenced by rotor RPM. The amplitude of flap deflection was found to reduce due to an increase in centrifugal friction and propeller moments with rotor RPM. In a subsequent experimental study of the concept using a Mach-scaled rotor model (Ref. 6), the authors noted an increase in the oscillatory rotor thrust due to a coupling between rotor blade modes and actuation frequency of the TEF. The authors were also able to reconfirm the degradation of flap performance with an increase in rotor RPM noted in their last study.

Leon and Gandhi (Ref. 7) have investigated the use of multiple spanwise trailing edge flaps for improvement of rotor performance, with a reported power reduction of 8% at high gross weight conditions through the use of these flaps. A subsequent reduction of rotor collective was also observed, which in conjunction with power reduction, will contribute to the expansion of vehicle flight envelope and increase the pilot's control authority. Gandhi (Ref. 8) has also explored the use of trailing edge flaps for primary flight control applications, thereby eliminating the need for a complex swashplate system, subsequently reducing the weight of the rotor hub. However, the authors reported a power penalty of 6-7% through this particular application of trailing edge flaps. It was not apparent in this study whether the weight reduction possible from a swashplateless rotor has been considered by the authors. Variable rotor RPM has also been explored by the authors, with a reduction in power demand noticed with a reduction of rotor RPM. As a result, the trailing edge flap deflection necessary for control has been found to increase.

Chen and Chopra have investigated the application of piezoceramic actuators for active twist applications aiming for a reduction in rotor vibration (Ref. 9). The authors have noted a net increase of 10% in rotor thrust from a 0.6 degree twist increase using piezoceramic actuators, with the local oscillatory lift increase being the highest when actuation frequency of blade twist actuators matched the rotor RPM. A reduction in twist amplitude has been noted by the authors with an increase in rotor RPM. Han et al. have investigated the use of dynamic blade twist for performance improvement (Ref. 10). The authors have found lower power reductions in hover and low speed forward flight as compared to high-speed flight using dynamic blade twist. The study also compares the use of the lower harmonic blade twist with higher harmonic blade twist, and the authors report larger power savings with the lower harmonic blade twist. In a subsequent study (Ref. 11), the authors have investigated the combination of variable rotor speed with variable blade twist. The authors have observed that the combination of the two techniques produces a larger power reduction ($\approx$ 23 %) as compared to that obtained from the use of a variable twist system alone ($\approx$ 3.3 %). The authors have argued that variable rotor RPM shows more performance benefits compared to the variable twist system alone. But through the combination of the two technologies, problems encountered by the application of variable speed rotors can be alleviated.

Camber morphing is a relatively new technique for helicopter rotors. From an aeromechanics perspective, this technique works similarly to trailing edge flaps. The primary difference between the two is that camber morphing employs pseudo-hinges instead of a separate flap on the trailing edge of the blade. As a result, any sharp discontinuities in the airfoil surface will be avoided, thereby preventing significant drag increase typically seen with trailing edge flaps. Figure 1 shows a comparison between a baseline airfoil shape and the airfoil after the application of camber morphing. In the context of fixed-wing aircraft, camber morphing has shown improvements in wing aerodynamic efficiency since camber modifications require minimal changes to the internal wing structure, while at the same time provide means for sufficient increase in wing performance (Ref. 12). Monner et al. also showed that for fixed-wing aircraft, the chord-wise camber variation leads to an improvement in operational flexibility

and performance (Ref. 13).

In the context of rotorcraft, extensive research is being undertaken to investigate the application of camber morphing to helicopter rotors. Roglin et al. have investigated the application of shape memory alloys (SMA) for active modification of airfoil camber in their research (Ref. 14). In this study, the conventional collective control of the helicopter has been replaced by the active camber modification system. The authors have noted that the SMA actuator requires less power as compared to a piezoelectric actuator for the same application. The SMA actuator was able to modify blade airfoil camber to an acceptable degree. This allowed a scaled helicopter model to climb from an initial hover state without requiring additional collective input from the pilot. In another study, Murugan et al. (Ref. 15) have investigated the use of curvilinear fibre composites for the development of the camber morphing skin of the blade, along with an internal skeleton for system actuation. Grohmann et al. (Ref. 16) have investigated the use of piezoceramic actuators for camber morphing targetted at the control of lift and pitching moment of the rotor blade sections. The authors have found the piezo-ceramic actuator performance to be satisfactory for this application.

The performance benefits of camber morphing are being investigated in the SABRE program (Ref. 17), along with the structural design and blade integration of various other morphing systems. SABRE program is an EU funded project investigating potential reductions in rotor power demand, engine fuel burn and emissions through the application of these rotor morphing technologies. Camber morphing is one of the many rotor morphing systems being considered in SABRE.

Variable speed rotors (VSRs) have been explored by various authors in the past in combination with different morphing systems (Ref. 8), (Ref. 11). Looking at the performance benefits of a VSR alone, it displays significant reductions in rotor power demand for medium and high-speed flight regimes (Ref. 18), (Ref. 19). Flight envelope expansion has also been observed using a VSR since drag rise due to compressibility on the advancing blade can be delayed. Therefore, the helicopter can fly faster keeping the engine power constant (Ref. 18). According to Xie et al. (Ref. 19), the VSR shows benefits at medium speed range primarily due to the reduction in profile power of the rotor blades, and at high speed due to the combined effects of the reduction in profile power and a delay in drag rise due to compressibility effects at the blade tips. However, the benefits at very low speed or hover are minimal since any gains due to profile power reduction are negated by the increased collective pitch requirement to maintain rotor thrust, which causes a subsequent increase in rotor power.

The combination of camber morphing with a variable rotor RPM has been explored in this study. It is hypothesized that the deficiencies of the VSR at low-speed flight and hover can be remedied through the use of camber morphing. In this regard, two distinct morphing systems will be investigated in this study, namely the active and the passive systems. It is necessary to note a difference in the terminology used in this study. Traditionally, active systems have been defined as those systems which attempt to modify rotor loads for various applications using higher harmonic control or similar methods, and are usually coupled to a closed-loop control system. The passive devices, on the other hand, have no such sophisticated control systems and rely on different methods to diffuse or isolate rotor vibratory loads. Passive devices suffer from limited bandwidth and high weight penalty, typically 3% of gross vehicle weight (Ref. 9). The active systems have a larger bandwidth, in comparison and lower weight penalty.

In this study, camber morphing systems have been classified based on their input power requirements rather than the system response. The active system requires external energy input for system actuation, whereas the passive system depends on the centrifugal forces prevailing on the blade for system actuation. Therefore, the passive system can only be controlled by varying the RPM of the rotor. This is a rather unique feature of the passive system, as the system will not require any additional input power for functioning. Whereas, the active system will require electrical or pneumatic power to be delivered to the camber morphing actuators.

Due to the unique control method of passive camber morphing, its combination with a VSR can be particularly beneficial for rotor performance in low-speed flight regimes. Morphing flaps of the passive system can be used to generate the additional force necessary to maintain thrust required to trim the vehicle when the main rotor is slowed down. This can be accomplished without significant increases in the collective pitch requirement of the rotor, which is the main source of the increase in power demand for the VSR for low-speed flight. The use of camber morphing will allow a local increase in lift, with a subsequent drag increase as well. But it is expected that there will be a net reduction in rotor power due to lower dynamic pressure experienced by the rotor with a lower RPM. Therefore, the combination of a VSR and camber morphing may prove to be beneficial for symmetrical and low-speed flight conditions. Henceforth, any discussion related to passive camber morphing will imply a coupling of the passive system and the VSR.

The performance of active and passive camber morphing systems will be analysed for hover and vertical climb flight conditions in this study. An attempt will be made to explore whether passive camber morphing can be used to remedy the deficiencies of the VSR. A comparison of active and passive camber morphing will be performed to understand which concept shows better performance benefits. The following sections describe the methodology used for numerical studies conducted for the assessment of camber morphing systems. First, the mechanical implementation and blade integration of the morphing systems have been discussed, followed by a description of numerical models used for the study, the baseline rotor geometry and flight conditions for which the camber morphing systems have been investigated. Next, results obtained from the numerical simulations have been

described in detail for each flight condition considered, after which some concluding remarks have been presented.

METHODOLOGY

It has been established in the previous sections that variable speed rotors do not show much benefit in terms of performance for low speed flight and hover conditions (Ref. 11), (Ref. 19). The main focus of this study is to understand whether rotor morphing can be used in conjunction with variable speed rotors such that the two systems become useful for symmetrical flight conditions like hover, where the VSR is found to be lacking in performance benefits. The hover condition is also one of the more power-intensive flight conditions in the operating envelope of the helicopter. Therefore, any significant performance benefits in this regime will affect the design of the helicopter as a whole. This is one of the main reasons why symmetrical flight conditions have been considered in this study.

From an aerodynamics perspective, these flight conditions have been identified as those where the variation of blade section aerodynamic properties such as angle of attack, Mach number, and aerodynamic coefficients, are negligible with respect to azimuth location on the rotor disk. The flow-field is symmetrical around the rotor shaft axis. Thus, these flight conditions would primarily encompass hover and vertical climb without forward motion. A second reason for consideration of symmetrical flight conditions is that the analysis in these flight regimes is straightforward and computationally less expensive as compared to forward flight. Therefore, this study will focus primarily upon hover and vertical climb conditions for trim and rotor analysis.

Camber Morphing

The coupling of camber morphing with the variable speed rotor opens up opportunities for the use of passive morphing systems for performance improvements in hover flight. The main differences between active and passive camber morphing are:

- **System Actuation and Applications:** Active camber morphing will require an external power supply for system actuation, typically in the form of electrical energy. Therefore, this system can be actuated at frequencies higher than 1/rev. The active system can be used for wider applications such as higher harmonic control, vehicle stability augmentation, vibration reduction etc. The passive system on the other hand can only be controlled by varying the RPM of the rotor, thereby allowing control in a quasi-static manner only. Therefore this system will be limited to the application of rotor power reduction or basic control augmentation only.
- **Blade integration:** While passive camber morphing possesses a limited range of applications, the actuators of this morphing system will be easier to integrate, as compared to the active system. Passive morphing actuators can be standalone devices incorporated inside the blade, and no external cables or connections to supply power will be necessary. The system can be actuated through the use of mechanical devices like springs. A schematic of such a design is shown in Figure 2. Other passive actuation methods like Von-Misses trusses (Ref. 20) can also be used. On the other hand, the active system will require cables or piping for delivery of electrical or pneumatic power to the actuators. This may also require significant modifications to the main rotor hub to make the system compatible with the rotor itself. Whereas, the passive system will only require the modification of the rotor blade, and not the entire rotor hub.
- **Power Demand:** Since active camber morphing requires an external power supply as mentioned in the previous section, there will be an additional power penalty through the use of this system, and the net power reduction (if any) will be lower than that achievable from the passive system for the same operating conditions and actuation range. On the other hand, the actuation of the passive morphing system will be based on the centrifugal forces prevailing on the blade, and no external power supply will be necessary. Therefore, passive camber morphing may allow larger power demand reductions for the main rotor.

The overall schematic of the camber morphing system and structural design of the trailing edge skin is similar for both the active and passive systems, as discussed in Ref. 21. The main difference between the passive system shown in Figure 2 and the active system is actuation mechanics. The passive system comprises of mechanical parts, mainly shafts and springs, subjected to centrifugal loads and are meant to cause the desired deflection of the skin whenever there is a change in rotor RPM. The flap is initially kept deflected to a desirable position. When the centrifugal force changes due to variation in rotor speed, Shaft 1 moves to initiate the linear movement of Shaft 2 which is connected to the trailing edge flap (shown in Figure 2). The flap deflection can be scheduled by the appropriate design of the portion of Shaft 1 that is linked to Shaft 2.

Blade integration issues mentioned above have been ignored in this study for both morphing systems being considered, and performance gains and envelope expansion for hover and vertical climb flight will be the only points of focus. In this regard, the two main parameters of importance for this study are the rotor power demand and collective pitch required to trim the helicopter for a given operating point. Rotor power demand is a direct measure of how camber morphing benefits the overall performance and fuel consumption of the vehicle.

The collective pitch will be looked at as an indirect measure of system performance, since it does not directly affect overall vehicle performance, but instead affects the pilot

control authority to a larger extent. For a constant collective pitch, camber morphing will allow an increase in rotor thrust, thus directly increasing the control authority available to the pilot. However, the use of collective pitch as a performance parameter significantly reduces the computational effort required in this study. The effect of camber morphing on rotor forces for fixed collective input has been discussed later to clarify this assertion. Therefore, reduction in power demand and collective pitch have been fixed as the primary performance parameters in this study. It should be noted that these parameters have been non-dimensionalized and then normalized using the rotor thrust coefficient when presented in the results section. This has been done to reduce the numerical error due to a relaxed tolerance of the trim algorithm.

Camber Morphing Effectiveness

The effectiveness of a morphing system can be defined as the degree to which the performance of the rotor is influenced by the actuation of the morphing system. Mathematically, effectiveness will be defined as the change in a particular performance parameter per unit deflection (or actuation) of the morphing system. The effectiveness of the camber morphing system depends on the location of the morphing flap on the blade, size of the flap, and rotor RPM. These three parameters in combination will determine how much force is generated by the morphing flap. Radial location and rotor RPM will primarily influence the dynamic pressure the flap operates in, and thus indirectly affect the force generated by the flap. The size of the flap directly affects the lift and drag forces generated by the flap. In this study, the rotor power demand and collective pitch requirement have been selected as the parameters of interest to properly gauge the performance of the camber morphing system. Correspondingly, two types of flap effectiveness parameters have been devised. These are:

1. **Power Effectiveness:** This parameter is essentially the change in power coefficient of the rotor per unit deflection of the camber morphing flap at a fixed RPM.

$$\zeta_P = \frac{\Delta(C_P/C_T)}{\Delta\delta_f} \tag{1}$$

2. **Control Effectiveness:** This parameter can be defined as the change in collective pitch per unit deflection of camber morphing flap for a fixed RPM.

$$\zeta_{\theta_o} = \frac{\Delta(\theta_o/C_T)}{\Delta\delta_f} \tag{2}$$

In equations 1 and 2 above, ζ_x is the effectiveness parameter, $\Delta(C_P/C_T)$ and $\Delta(\theta_o/C_T)$ are the changes in the respective rotor performance parameter and δ_f is the flap deflection angle in degrees. These parameters have been defined such that negative values for these parameters may be encountered. This can be explained by the fact that the performance parameter under consideration has a lower value than the reference value of the parameter at zero flap deflection. Accordingly a larger negative value translates to better performance achievable from camber morphing for a particular morphing flap deflection. In comparison, a small positive value means degradation in the performance of the rotor due to camber morphing, since the power demand or collective pitch requirement is higher than that of the baseline condition.

The collective pitch has been used as an indirect measure of performance comparison in this study. If the collective pitch is kept constant, the deflection of the camber morphing flap will result in a local increase of lift and drag. The net result will be an increase in rotor thrust with some additional power penalties. But in this situation, the rotor will no longer be trimmed. Computation of rotor power and collective are possible from the same numerical analysis. Whereas, the analysis of an increase in rotor thrust will require additional computational effort. The expected increase in rotor thrust when the collective input is kept fixed has been analysed for one representative flight condition.

The two effectiveness parameters have been used to determine the size and location of the camber morphing system on the rotor blade. These parameters will also be instrumental for comparison of the performance of the passive camber morphing system when the RPM of the rotor is varied or different flight regimes are encountered. The detailed results of the placement of the morphing flap on the rotor blade have been discussed with other results.

Numerical Models

At the start of the SABRE program (Ref. 17), it was ascertained that a new conceptual design tool for helicopters must be developed, which can cater to the unique requirements of assessment of morphing systems, and their influence on the design of the helicopter from a system-level perspective. The tool will also be required to recommend design changes to the vehicle in response to rotor morphing. Moreover, a tool that includes rotor morphing in its design algorithms would provide additional freedom to the designers during the conceptual design phase. These factors lead to the creation of HOPLITE. This tool has been used for the numerical analysis of camber morphing systems performed in this study. The tool has been described in more detail in Ref. 22.

HOPLITE has been developed as a low fidelity tool for flight mechanics analysis since the higher fidelity levels provided by for example CFD algorithms for aerodynamics are deemed unnecessary at the conceptual design stage. Moreover, these algorithms will be computationally expensive with large processing time requirements. HOPLITE's algorithms have been developed to provide the necessary resolution required for analysis of candidate morphing systems, and at the same time enabling low computational resource requirements and fast processing

speed. A description of the most important models and algorithms of the tool for this study is provided next.

The rotor model of the tool is the most important one from a morphing system analysis perspective. This model utilizes Blade Element theory with modifications so that local changes in blade geometry due to rotor morphing can be captured with acceptable fidelity. The rotor model also features a variable inflow model (Pitt-Peters 3 state model (Ref. 23)), tip loss corrections, and look-up table based estimation of airfoil aerodynamic coefficients for un-morphed airfoil sections. When the blade shape changes in response to camber morphing, the MSES aerodynamic solver (Ref. 24) is utilized to obtain aerodynamic coefficients for these modified shapes. It was initially considered to parametrize the effect of camber morphing by correcting the baseline airfoil look-up tables using a ΔC_x parameter added to the baseline coefficients, where C_x is the relevant aerodynamic coefficient. But this exercise was found to be unreliable due to changes in blade section Mach and Reynolds' numbers in response to variable rotor RPM. Therefore, MSES was coupled to the rotor model for airfoil analysis for sections where camber morphing is active.

The rotor model also features a low fidelity aeroelastic model. This model assumes a torsionally stiff blade with a constant mass distribution along the span. Since the morphing actuators have not been integrated with the blade yet, the model ignores the changes in the local mass distribution of the rotor blade. The high torsional stiffness of the blade results in the camber morphing system utilizing the direct lift effect (described by Friedmann (Ref. 1)) to modify the local aerodynamics of the rotor. Blade flap dynamics and motion about the flap hinge are modelled by assuming a spring of appropriate stiffness placed at the blade root. Due to the various simplifying assumptions made, higher-order aeroelastic effects like pitch-flap coupling and changes in the blade twist in response to camber morphing are ignored by the aeroelastic model.

HOPLITE features a 3 degree-of-freedom rigid body model for trim purposes. The trim algorithm iteratively computes the accelerations ($\dot{u}$ in the longitudinal direction, $\dot{w}$ in the vertical direction) and angular rates ($\dot{q}$ as pitch rate) of the vehicle. Vehicle controls such as collective pitch (θ_o), longitudinal cyclic (θ_{1s}) and fuselage pitch (θ_f) are computed by the trim algorithm to minimize the accelerations. Accelerations and angular rates in all other directions are assumed to be zero, and therefore the corresponding controls are assumed to be frozen by the algorithm. This allows HOPLITE to perform a rudimentary, quasi-steady mission analysis of the complete vehicle. It should be noted that in equations 1-2 the performance parameters have been normalized using the rotor thrust coefficient. This is to reduce the numerical error in rotor forces which occurs due to the tolerance setting of the trim algorithm. With a tighter tolerance value, the trim algorithm takes longer to minimize vehicle accelerations thereby increasing the convergence time. A more relaxed tolerance results in quicker convergence, but the numerical error in rotor forces is also higher, although still within acceptable limits. Therefore, normalization using the thrust coefficient works towards the minimization of this numerical error.

For this study, only hover and vertical climb flight conditions have been considered. In future investigations when camber morphing is activated for forward flight as well, it will be possible to estimate its effect over the entire mission profile. This will allow HOPLITE to ascertain the necessary design changes in the baseline vehicle in response to rotor morphing. However, these aspects have not been covered in this study.

Rotor Geometry

The MBB Bo-105 helicopter was selected as the reference vehicle for the SABRE program (Ref. 17). Therefore, this study will also use the same reference helicopter for various numerical simulations. As mentioned previously, a full mission profile analysis of the camber morphing has not been conducted in this study. Therefore, the baseline design parameters of the Bo-105 have not been modified. However, rotor geometry does change in response to camber morphing. The geometrical parameters of the baseline rotor blade are described in table 1, as reported by Rauleder et al. (Ref. 17). Camber morphing systems have been incorporated into the rotor blades between 70-90% radius. The span of the morphing flaps has been selected to be equal to 20% radius, and the chord length of the flap has been set at 25% of local blade section chord. The dynamic pressure at this location on the blade is sufficient to keep the effectiveness of the morphing flap at a high level, and the actuation of the flap will have a substantial impact on the local aerodynamics of the rotor. This will result in the improvement of various rotor performance metrics.

The airfoil shapes at the location of the morphing system have been modified from the baseline NACA 23012 airfoil. The modification of the airfoil is automated by HOPLITE. The mean camber line of the airfoil is modified first in response to the input flap deflection and hinge line location of the flap. The hinge line of the flap has been kept fixed at 75% chord for all numerical analyses performed in this study. The mean camber line is modified using a Bezier curve implementation, thereby ensuring that no sharp discontinuities are present in the camber line. Next, the upper and lower surfaces of the airfoil are recomputed by maintaining the thickness distribution of the baseline airfoil with respect to the chord. This ensures that the airfoil shape upstream of the hinge line remains the same as that of the baseline airfoil. The transition between baseline and morphed airfoil shapes is assured to be smooth using this method. A comparison between the baseline airfoil shape and the modified airfoil shape is shown in Figure 1.

Description of Flight Conditions

As discussed in the previous sections, rotor morphing systems show maximum performance benefits at the edge of

the flight envelope. Since this study is limited to the vertical flight regime, three flight conditions have been considered to fully understand and quantify the performance of the camber morphing systems. Two hover conditions, one at sea-level and another at an altitude of 2000 meters, as well as vertical climb at zero forward speed have been used for the analysis of active and passive camber morphing systems.

The first flight condition has been considered to establish the baseline performance of the morphing system, and to check whether the numerical models used possess sufficient fidelity to capture the changes in local aerodynamics of the blade due to camber morphing. The other two flight conditions have been considered to explore the performance of camber morphing at or near the edge of the flight envelope and to verify whether the use of camber morphing indeed shows larger performance benefits for these operating points. The details of these flight regimes are shown in table 2. The helicopter is assumed to operate at standard temperature and pressure conditions, and hot and high operating conditions have not been analysed in this study.

The analysis of the morphing systems has been limited to 3 rotor RPM settings. These are 100% nominal RPM, 95%, and 90% RPM. At 100% RPM, both the active and passive systems are assumed to be operational, and at other RPM settings, only the passive system is activated. Table 3 shows a test matrix with different flight conditions and RPM settings for which a particular type of morphing system has been analysed. Since blade integration of the morphing systems has not been performed yet, the 100% RPM case can be used to describe the performance of both the active and passive systems. The lower RPM limit for the passive system has been set at 90%. The most important consideration for this decision is the resonance between the rotor and the structural components of the vehicle. If the rotor RPM matches the resonant frequencies of vehicle structural components, catastrophic failure can occur since resonance between the structure and the rotor is more likely to occur below 90% RPM. The analysis of camber morphing for fixed collective input has also been performed for sea-level hover at 100% RPM. The results of the analysis of camber morphing for the flight conditions described are detailed in the next sections.

RESULTS

The initial analysis of camber morphing systems relates to the position and size of the morphing flaps. Power effectiveness (ζ_P) and Control effectiveness (ζ_{θ_o}) have been used for comparison of rotor performance for this analysis. Once the two geometrical parameters of the morphing system have been established, a more detailed rotor analysis has been performed for the three flight conditions described above.

Morphing System Placement

The size and placement of the morphing system on the rotor blade are important considerations for the proper understanding of system performance. The flap deflection was kept constant for this analysis and was chosen such that the effect of the camber morphing could be clearly seen on rotor power and collective demand. A lower deflection than what was selected resulted in very minute differences in power and collective and a very large flap deflection caused a large increase in profile drag, thereby nullifying any possible performance benefits. Therefore, this investigation was performed for sea-level hover conditions, for a fixed camber flap deflection of 3 degrees.

The results of this analysis are shown in Figure 3. The figure shows the variation of morphing system effectiveness parameters ζ_P and ζ_{θ_o} with flap location on the rotor blade. The flap location shown in the figures signifies the radial position of the starting section of the camber morphing system on the rotor blade. As mentioned before, by definition, the effectiveness parameters can take negative values, which indicates that the rotor has been trimmed at a lower collective pitch or has a lower power demand from the use of camber morphing.

A comparison of two flap geometries has also been made in Figure 3. For this analysis the morphing flaps have been moved progressively outboard. The primary difference between the two flap geometries is the length of the morphing flap. One design features a flap of length equal to 20% rotor radius (1 meter length for the reference rotor), and the other design has a flap with length equal to 10% rotor radius. Other parameters like deflection range, and flap chord length are essentially the same for both designs.

Figure 3a shows a comparison of control effectiveness for the two different configurations. The key observations from this figure are:

- The rotor equipped with a camber morphing flap with a smaller length requires a larger collective pitch to trim as compared to one with the larger flap regardless of the position of the flap.
- The control effectiveness of both configurations improves as the flaps are moved outboard. The rotor with a larger flap shows rapid improvement in control effectiveness as the flap is moved outboard, with the maximum effectiveness seen at the most outboard location.

Figure 3b shows a similar trend for variation of power effectiveness with radial location for the two morphing flap configurations.

The primary factors influencing the performance of the flaps are the dynamic pressure on the flap and the surface area of the flap. As the flap is moved outboard, the dynamic pressure on the flap increases, which directly influences the force generated by the flap. Additionally, a larger flap length translates to a larger flap surface area, which also contributes to an increase in forces generated by the flap. These two factors result in a direct increase of lift at the position of the flap. This leads to a reduction in the collective pitch required

to trim the rotor and the average angle of attack seen by the rotor blade. Therefore, this leads to a reduction in rotor power as well. The reduction of collective pitch and power demand is evident from Figure 3. A larger flap may also have other potential benefits since a multi-segmented flap can be created for further performance improvements.

Looking at these results, the position of the camber morphing flap has been fixed at 70%-90% radius on the blade from the centre. Placing the flap further outboard only shows a minor reduction in power ($\approx$ 0.3%). Additionally there will be a subsequent increase in the centrifugal forces on the system, thereby requiring a heavier and more complex design to function adequately.

Effect of Camber Morphing on Aerodynamic Coefficients

The incorporation of camber morphing systems within the rotor blade is aimed at modifying and controlling the local aerodynamic parameters of certain blade sections to fulfil various purposes. Camber morphing flaps can be used to locally increase lift, and hence additional thrust can be generated by the rotor. This will help in the reduction of collective pitch required to trim the rotor for a specific flight condition. If the collective is kept fixed, the additional thrust generated will allow an increase in pilot control authority. The effect of camber morphing on local blade section aerodynamics is shown in Figure 4. This investigation has been performed for airfoil sections in the central region of the camber morphing flap at a radial location of 80% radius. The Reynolds and Mach numbers have been kept constant at $3.27X10^6$ and 0.514 respectively for this analysis. The angle of attack range studied is typical of values observed on the rotor blade at this radial location. Therefore, only a limited range of angles of attack have been considered.

Figure 4a shows the variation of lift coefficient with angle of attack (α) for increasing flap deflection. The variation of lift coefficient (C_l) is largely linear in the angle of attack range studied. Since large negative or positive angles have not been considered, the airfoil does not stall in this range. It is interesting to note that the lines for lift coefficient for different flap deflections are largely parallel over the angle of attack range studied. For a zero α, an increase in C_l of about 130% is observed when going from zero flap deflection to a 5 degree flap deflection. This increase is also noted over the entire angle of attack range. Considering the zero lift angle of attack of the airfoil section, it can be seen that for zero flap deflection, zero lift occurs at a -1.2 degree angle of attack. As the flap deflection is increased, zero lift angle shifts to progressively lower angles of attack, shifting to -3 degree for a 5 degree lap deflection. These effects essentially mean that the airfoil will be able to generate positive lift for an increasing range of negative angles of attack, as well as generate more lift over the entire α range.

Figure 4b shows the variation of airfoil drag coefficient (C_d) with angle of attack for various flap deflections. In this case, the variation of the drag coefficient is non-linear. For high angles of attack, there is a drastic increase observed in drag coefficients for all flap deflections. Additionally, the drag coefficient begins to rise a lot sooner as the morphing flap deflection is increased. For negative angles of attack, it can be observed that a larger flap deflection shows a lower drag coefficient. But since these angles of attack are rarely encountered by blade sections placed at 80% radius, this reduction of drag coefficient does not have any effect on rotor power demand. It should also be noted that moderate angles of attack, typically below 4 degrees, are seen at the location of the morphing flaps. This ensures that large drag coefficients are not observed by the morphing flaps. Therefore, the drag coefficients encountered will largely be in the linear regions of the polar.

The overall effect of camber morphing on local airfoil aerodynamics is clear. There is a significant increase in lift coefficient with increasing flap deflection. Correspondingly, there is also an increase in the drag coefficient observed. This would mean that local thrust and power coefficients will be higher than those observed for zero flap deflection. However, the additional thrust generated will allow for a lower collective pitch, and a subsequent reduction of the average angle of attack of the blade sections may also be observed. This will be beneficial for the overall rotor performance.

Hover at Sea-Level

This flight condition is the most important from numerical analysis and validation perspectives. This condition has been used as a test case to verify whether HOPLITE's rotor model has sufficient fidelity to model the changes in local aerodynamic properties seen on the blade due to rotor morphing. In this regard, a deeper investigation of flow conditions prevalent on the rotor has been performed for this flight condition. The changes in blade section angle of attack and aerodynamic coefficients in response to camber morphing and variable rotor RPM have also been considered.

Changes in local aerodynamics due to camber morphing
The changes in local aerodynamic properties have been shown in Figures 5 - 7. Each polar plot shows the distribution of a particular aerodynamic property varying along the blade for a fixed morphing flap deflection. Since the flow is symmetric about the rotor shaft, the plots are also symmetrical about the origin. The RPM has been kept constant at 100% nominal (=424 RPM for the reference rotor) for this analysis so that the effect of camber morphing alone can be properly understood.

Figure 5 shows the local angle of attack distribution on the rotor disk and its variation with increasing morphing flap deflection. At zero flap deflection, it can be noted that the blade sections between 40% and 80% rotor radius operate at the larger angles of attack compared to the root and tip sections. This is due to a combination of induced velocity and the twist of the rotor blade, as described in Table 1. As the deflection of the morphing flap is increased, the local

blade section angle of attack starts reducing. The maximum angles of attack for each azimuth location are seen by sections situated between 40-80% radius on the rotor disk for all flap deflections. It has been observed that these maximums reduce from upwards of 3 degrees to below 2.4 degrees when the morphing flap deflection is increased from zero to 5 degrees. This reduction can be attributed to the fact that an increase in flap deflection generates additional thrust force, and a lower collective pitch is then sufficient to trim the rotor for the given flight condition.

The lift and drag coefficient distributions on the rotor disk are directly affected by changes in the local angle of attack, the shape of the airfoil section, and the dynamic pressure. Since camber morphing directly influences the shape of the airfoil, this will have a significant impact on the lift and drag coefficient distribution on the rotor disk. This is evident from Figures 6 and 7.

It can be seen from Figure 6 that as the morphing flap deflection is increased, the lift coefficients for sections positioned in 70%-90% radius range show a significant increase over other blade sections. This effect is clearly visible as the flap deflection is increased beyond 3 degrees, with a band of high lift coefficient becoming prominent. This is the direct result of camber morphing. Another less prominent but important effect which can be observed from Figure 6 is the reduction of lift coefficient on the blade tips and sections outboard of the morphing flaps. This apparent unloading of blade tips is important from an induced power perspective and can be attributed to the reduction in local angle of attack seen in Figure 5. The reduction of induced power in these blade sections directly contributes to the reduction of rotor power demand.

Figure 7 shows the local drag coefficient on the rotor disk and its variation with increasing flap deflection. Two important observations can be made from this figure. Firstly, there is a noticeable drag increase with increasing flap deflection for blade sections located in 70-90% radius range. This is expected since the drag coefficient will increase with an increase in the lift coefficient due to camber morphing. However, a reduction in the drag coefficients on the blade tips can also be observed. This is due to a reduction in local angle of attack on the blade tips due to camber morphing. This reduction in drag coefficient is very important since the blade tips operate at maximum dynamic pressure as compared to other sections. Therefore, a reduction in drag coefficient for these sections will have a large positive impact on the rotor power demand. The increase in drag coefficients noticed for the morphing flaps is compensated for by the reduction drag coefficients on the blade tips. Therefore, an overall reduction in rotor power demand is possible.

Changes in local aerodynamics due to variation of RPM The variation of local aerodynamics in response to variation of RPM for a fixed morphing flap deflection is shown in Figures 8 - 10. Two flap deflections have been chosen for this analysis to explore whether the combination of particular RPMs and flap deflections can be used to optimize rotor performance. Therefore, flap deflections of 3 and 5 degrees have been selected for this analysis.

Figure 8 shows the distribution of the blade section angle of attack around the rotor disk. For a reduction in rotor RPM, an increase in the local angle of attack all around the disk can be observed from the figure. This can be attributed to the increase in collective pitch required to trim the rotor due to a reduction in dynamic pressure. The reduction in rotor forces due to RPM reduction can be compensated by the increase in forces due to the higher collective pitch. It can also be seen from Figure 8 that it is possible to obtain the same local angle of attack distribution for two different RPMs. The combination of 3 degree flap deflection with 100% RPM results in a distribution very similar to that seen with 5 degree flap deflection at 95% RPM. Therefore, with a proper combination of rotor RPM and morphing flap deflection it may be possible to optimize the performance of the rotor to a large extent.

Figures 9 and 10 show the variation of local lift and drag coefficients respectively with varying RPM for two flap deflections. The increase in the local angle of attack due to a reduction in rotor RPM is the dominant factor governing the variation of these coefficients. Therefore, a consequent increase in local lift coefficients is observed in Figure 9 as the rotor RPM is reduced for a fixed flap deflection. This is due to an increased collective pitch requirement to trim the rotor with a reduction in RPM. The situation where the angle of attack distribution is similar for two different rotor RPMs seen in Figure 8 is not seen for lift coefficient distribution though. This is due to the difference in flap deflections for the two different RPMs considered. The larger flap deflection will naturally result in larger local lift coefficients for the blade sections where the flaps are placed.

Figure 10 shows the distribution of drag coefficients on the rotor disk for varying RPM. For constant flap deflection, it can be noticed that with the reduction of RPM, the blade tips operate at lower drag coefficients. This can be attributed to the reduction of Mach number seen by these blade sections. On the contrary, the inboard sections see an increase in drag coefficients. The increase of drag on the inboard sections is largely due to the increase in collective pitch from the reduction of RPM. Even though the drag on the inboard sections of the rotor has increased, a reduction of drag on the blade tips has a greater impact on rotor power demand. Therefore, a net reduction of power demand can be observed due to a reduction in rotor RPM. The distribution of the drag coefficient for the increased flap deflection for the same rotor RPM follows a trend similar to lift coefficient distribution, and higher drag coefficients are observed for blade sections equipped with morphing flaps.

Overall rotor performance The overall performance of the camber morphing system for sea-level hover conditions has been shown in Figure 11. A decreasing trend is observed in the collective pitch required to trim the rotor as the deflection

of the morphing flap is increased. This trend is seen for all 3 RPM settings analysed, as evident from Figure 11a. A maximum reduction of nearly 12% is seen for the collective pitch. This can be attributed to the extra force generated by the morphing flap as its deflection is increased. Therefore, a lower collective pitch will be sufficient to generate the thrust force necessary to trim the rotor. The reduction of collective control is an indirect measure of an increase in control authority. However, the change in rotor thrust for constant collective gives a better overview of the increase of control authority. This has been addressed in the next section.

Only minor changes are observed in rotor power demand with an increase in flap deflection, typically less than 1% as seen in Figure 11b. This observation is as expected since previous studies have also noted that rotor morphing may be effective only at the edge of the flight envelope where large angles of attack are seen of the rotor blade. A larger reduction in power demand is seen with a reduction in rotor RPM as compared to that seen with flap deflection, approximately 3% by reduction of RPM. The sudden variations observed in the power demand (95% RPM line in Figure 11a) have been attributed to numerical errors due to the relaxed tolerance of the rotor trim algorithm.

Changes in rotor forces for fixed collective Figure 11a has shown a large reduction in collective pitch required to trim the rotor through the use of camber morphing flaps. This can be indirectly translated to an increase in the control authority of the pilot through the use of camber morphing. A more direct measure of this increase in control authority can be observed if the collective pitch is held constant as the flap deflection is increased. The maximum thrust generated by the rotor will increase drastically, thereby increasing pilot control authority for a given flight condition. This analysis has been performed for hover at sea-level, and the collective pitch input has been kept constant at 7.5 degrees. The results of this analysis are shown in Figure 12.

For a fixed collective input as the flap deflection is increased, the morphing flap will be able to generate additional lift, with a corresponding increase in drag. Therefore, if the collective is kept fixed, there will be a net increase in both rotor thrust and power demand. Figure 12 shows the variation of thrust and power coefficients with an increasing morphing flap deflection. From the figure, an increase of 10% in the rotor thrust coefficient is observed, with a 12% increase in power coefficient for the same range of flap deflection. The large increase in rotor power demand can be attributed to the fixed collective input. Since the average angle of attack of the rotor blade is no longer allowed to change, the drag coefficients of blade sections other than the morphing flap are more or less constant. Therefore, there is no reduction of power observed for a fixed collective input.

The unloading of rotor blade tips observed for a constant thrust coefficient seen in the previous analysis is also not observed here. Therefore, any related compensatory affect on power reduction will not be observed for this case. Nevertheless, the increase in the rotor thrust observed is significant. This means that there is more thrust available to the pilot without the requirement of additional control input. As a result, expansion of the flight envelope is possible through the use of camber morphing, with a positive effect on the hover ceiling and service ceiling of the helicopter.

Looking at the changes in the local angle of attack distribution in Figures 5 and 8, camber morphing will indeed be beneficial for flight conditions where high angles of attack can be observed. Through a lower collective pitch demand, camber morphing will be able to reduce the angle of attack seen by the blade sections, thereby preventing blade stall and associated drag penalties. For sea-level hover, such high angles of attack are not encountered. Therefore, power benefits are minimal. Nevertheless, the use of camber morphing does reduce the collective pitch required to trim the rotor, thus providing more control authority to the pilot for a given manoeuvre.

Since the flow-field is symmetrical around the rotor shaft for the flight conditions analysed in this study, the trends observed in Figures 5 - 10 will also be seen for other flight conditions. Therefore, the discussion of these figures will be limited to the sea-level hover condition only.

Vertical Climb

In the previous section it was established that camber morphing may show larger performance benefits for flight conditions in which the blade sections encounter high angles of attack, or for operations at the edge of the flight envelope. Vertical climb without forward speed is one such condition. This condition is expected to require a larger collective pitch input and power demand as compared to sea-level hover. A comparison of collective pitch requirements between sea-level hover and sea-level vertical climb condition can already be made from Figures 11a and 13a. Indeed the vertical climb condition requires a larger collective pitch input and therefore higher average angles of attack on the rotor blade. Thus, camber morphing may already show larger benefits for this flight condition. Various parameters that define this flight condition, such as altitude, rate-of-climb, forward speed etc., have been described in Table 2. Note that in the table, a flight path angle of 90 degrees has been specified. This means that the vehicle is not moving forward, but only vertically upwards. A detailed analysis of local flow-field distribution has not been presented for this case due to its symmetry about the rotor shaft axis. The overall performance of the morphing systems for this case has been presented in Figure 13.

Figure 13a shows the variation in collective pitch required to trim the rotor with increasing morphing flap deflection for vertical climb flight. The reduction trend observed for collective pitch requirement in hover condition is also seen for this flight condition. The percentage reduction of the collective is nearly the same for both hover and vertical climb ($\approx 10\%$). The large non-linear jumps in collective pitch and

rotor power demand have been attributed to the numerical error due to a lower tolerance of the rotor trim algorithm.

The variation of the rotor power coefficient seen in Figure 13b does not follow the trend shown for hover condition. For the vertical climb condition, a maximum reduction of 3.5% is observed for constant rotor RPM. Whereas for the hover condition, the observed reduction in power coefficient was below 1% (from Figure 11b). Therefore, for this flight condition, in addition to a reduction in collective pitch, the use of camber morphing also enables a reduction of rotor power demand. It should be noted that the climb velocity was fixed at 7 m/s for this case. A larger performance benefit may be obtained for a more aggressive vertical climb manoeuvre. As seen for sea-level hover case, a larger reduction in power is observed by reducing the rotor RPM ($\approx$ 6.5%) as compared to increasing the deflection of the morphing flap for a fixed RPM ($\approx$ 3.5%).

Hover at Altitude

Hovering at a high altitude is another operating condition encountered in the normal flight envelope where high angles of attack may be seen on the rotor disk for some blade sections. Parameters which define this operating condition are described in Table 2. This flight condition is also affected by a lower dynamic pressure than that encountered at sea-level due to a reduction in the density of air. Therefore, a larger collective pitch is required for this operating point as compared to sea-level hover to compensate for the reduced dynamic pressure. This increase in collective pitch can also be verified from Figures 11a and 14a. Hovering at altitude indeed requires a larger collective pitch, and hence a larger average angle of attack will be seen by rotor blade sections.

Figure 14 details the overall performance of the rotor for hovering at 2000 meters altitude. A detailed analysis of the flow field and distribution of aerodynamic coefficients has not been performed for this case since the flow field is largely symmetrical about the rotor shaft axis. Figure 14a shows the variation of the collective pitch with increasing deflection of the camber morphing flap. This trend of reduction in the collective with increasing flap deflection is also seen in Figure 11a. However, a larger reduction, approximately 14%, is obtained for hover at altitude, as compared to hover at sea-level, which shows a reduction of about 10% only. Therefore camber morphing seems to provide a larger control authority gain for this flight condition.

The reduction in rotor power through the use of camber morphing for hover at altitude is also found to be larger for this case as compared to sea-level hover. Figure 14b shows the variation in power coefficient for this condition. The maximum reduction in power coefficient is found to be nearly 6% for high altitude hover with constant RPM as compared to less than 1% for sea-level hover. Thus, camber morphing is again found to have larger performance benefits at the edge of the flight envelope. However, as seen for other flight conditions, a reduction in rotor RPM seems to provide larger power reductions as compared to increasing the deflection of the morphing flap. While hovering at 2000 meters, rotor RPM reduction shows a power coefficient reduction of approximately 9.5%, as compared to 6% by increasing the deflection of the morphing flap.

At the outset, it was hypothesized that camber morphing alone may not be useful from a performance perspective. However, in combination with a variable speed rotor, the two concepts may provide larger performance benefits. This hypothesis has been verified in this study. Reducing rotor RPM shows larger power reductions as compared to the use of morphing flaps for all flight conditions investigated. Additionally, camber morphing reduces the collective pitch input required to trim the vehicle. Considering hover at 2000 meter altitude, the collective pitch required to trim the rotor at 100% nominal RPM and zero degrees flap deflection was found to be the same as that obtained for 95% nominal RPM and 5 degree flap deflection. A collective input of approximately 9 degrees was needed for both conditions. The power reduction for these two combinations of RPM and flap deflection was found to be nearly 5.5%. Thus, for the same control input, a combination of rotor RPM setting and flap deflection can be found where a net reduction in power can be obtained. A proper scheduling of RPM and flap deflection can yield larger performance benefits, but this analysis has not been performed in this study and will instead be the subject of future work.

Comparison between Active and Passive Camber Morphing

After looking at all three flight conditions, a comparison between active and passive camber morphing can now be easily performed. Hover at 2000 meters altitude is good flight condition for this comparison. This flight condition has been chosen since the rotor is operating at or near the edge of the flight envelope, and maximum performance benefits have been seen for this operating point. Figure 14 shows the performance of both active and passive camber morphing for this flight condition. The active system is represented by the 100% RPM lines in the plots. It should be remembered that the active system is only functional at 100% RPM (Table 3). Whereas the passive system has the freedom to operate at all RPMs. Considering the baseline condition at 100% RPM and zero flap deflection, the following observations can be made:

- The maximum power reduction for the active system at full flap deflection is found to be 5.8%, and a reduction in the collective pitch of 14% is observed.
- For the passive system, a maximum power reduction of 10.4% is found to occur at 6 degree flap deflection and 90% RPM, with a similar reduction in collective pitch as seen for the active case.

The blade integration of the two systems has not been performed and therefore has been ignored in this study. Since

the active system will require additional power input for actuation, the net power gain from this system will be lower than that obtained from a pure aerodynamic analysis in this study. Even when the parasite power demand of the morphing systems has not been accounted for, the passive system outperforms the active one from a power-saving perspective. Therefore, overall a larger performance benefit can be obtained from the passive camber morphing system as compared to the active system.

CONCLUSIONS

This study focused upon the feasibility of camber morphing systems for helicopter rotors for symmetrical flight conditions. The performance of two different types of camber morphing systems, the active and passive systems, were analysed for hover at sea-level, vertical climb and hover at a high altitude. It was hypothesized that the passive morphing system, which combines camber morphing with a variable speed rotor, will show larger performance gains. Two main parameters were considered for performance comparison of the morphing systems. These were the rotor collective pitch and power coefficient. The following conclusions can be made from this study:

1. A comparison of different positions for the placement of the morphing flap on the blade showed that the flap will be most effective when placed at the 70-90% radius location. A larger flap with length equal to 20% blade radius was found to be more effective as compared to one with a smaller length of 10% blade radius. Therefore, the analysis of active and passive morphing systems has been performed with a flap of length 20% radius placed at 70-90% radius location.

2. Analysis of the aerodynamic characteristics of the morphing flap airfoil section for a fixed Reynolds and Mach number shows a significant increase in lift and drag coefficients of the airfoil section when the morphing flap deflection is increased. This leads to a local increase in thrust as well as power demand. But the increase in thrust allows a reduction in collective pitch, which results in the overall rotor thrust remaining the same and a net reduction in rotor power demand is then possible.

3. A detailed investigation of the flow-field and distribution of aerodynamic coefficients on the rotor disk was performed for sea-level hover condition. For a constant rotor RPM, it was observed that increasing the deflection of the morphing flap resulted in a reduction of rotor collective pitch due to additional thrust generated by the flap. This lead to a reduction in the average angle of attack seen by the blade sections. Consequently, the lift coefficient was found to reduce on the blade for all blade locations other than those where the morphing flaps are placed. This resulted in a reduction of rotor induced power. The drag coefficient at the blade tips was also found to reduce due to a lower angle of attack. This resulted in a reduction of rotor profile power.

4. The effect of reducing the rotor RPM was analysed for two flap deflections. A reduction in RPM increased the average angle of attack seen by the blade sections due to an increase in the collective pitch required to trim the rotor. This increased local lift and drag coefficients. However, a reduction in dynamic pressure due to lower RPM caused a reduction in rotor power demand.

5. The overall performance analysis of camber morphing for hover condition showed a reduction of 10% in rotor collective pitch, which increased the control authority available to the pilot. However, only minor power reductions were noticed for a full deflection range of the morphing flap for constant RPM. The overall effect of camber morphing is the reduction of the average angle of attack seen by the blade sections. Therefore, the technique may be more beneficial for flight conditions where higher angles of attack are witnessed.

6. On analysis of rotor forces for a fixed collective input, it was observed that the rotor thrust increased by approximately 10% through the use of camber morphing. This resulted in a direct increase in pilot control authority, as well as an expansion of vehicle flight envelope. This additional thrust generated may have a positive effect on the hover and service ceilings of the vehicle as an example. An increase in rotor power demand was also observed for fixed collective input.

7. The overall performance analysis of morphing flaps for the vertical climb manoeuvre showed larger reductions in power as compared to hover at sea-level. The collective pitch required to trim the rotor is higher than that at sea-level hover. Therefore, higher angles of attack will be seen by the blade sections. Through the use of camber morphing, a larger reduction in the rotor power demand, nearly 3.5%, was observed for constant RPM for this flight condition as compared to the sea-level hover condition. The reduction in collective pitch was nearly the same for both conditions.

8. The analysis of the performance of the morphing system for hover at high altitude condition showed larger collective and power reductions as compared to the other two conditions analyzed. A power reduction of 6% was observed for this flight condition for a constant rotor RPM. This is significantly higher for hover at sea-level. A collective pitch reduction of 14% was also observed in this case. Therefore, camber morphing shows larger performance benefits for operating conditions at or near the edge of the flight envelope as compared to normal operating points like hover at sea-level.

9. Comparing the performance gains achievable from camber morphing and variable speed rotors

independently, larger performance gains have been obtained from the latter. However, this comes at a penalty of higher collective pitch required to trim the rotor at lower RPMs. When camber morphing systems are coupled to the variable speed rotor, the collective pitch requirement reduces, since morphing flaps can compensate for the reduction in collective. This phenomenon can be used for further optimization rotor performance by finding good combinations of RPM and flap deflection.

10. Passive camber morphing has been found to show larger performance benefits as compared to active morphing due to the combination of the reduction in rotor RPM and camber morphing. A higher reduction in rotor power, as well as collective pitch, has been observed with passive camber morphing. Reductions in the order of 10% in the power demand were obtained for the passive system at 90% RPM and maximum flap deflection. The reduction in rotor RPM is the primary reason behind the performance benefits of the passive system.

Author contact:
Kushagra Vidyarthi - K.Vidyarthi@tudelft.nl;
Yasir Zahoor - Y.Zahoor@tudelft.nl;
Marilena D Pavel - M.D.Pavel@tudelft.nl;
Roeland De Breuker - R.DeBreuker@tudelft.nl;
Mark Voskuijl - m.voskuijl@mindef.nl

ACKNOWLEDGMENTS

This work was funded in part by the European Research Council (ERC) under the European Union's Horizon 2020 research and innovation programme, as part of the Shape Adaptive Blades for Rotorcraft Efficiency (SABRE) programme (grant agreement No 723491).

REFERENCES

1. Friedmann, P. P., "On-Blade Control of Rotor Vibration, Noise, and Performance: Just Around the Corner? The 33rd Alexander Nikolsky Honorary Lecture," *Journal of the American Helicopter Society*, Vol. 59, (4), 2014, pp. 1–37.

2. Kerho, M., "Adaptive Airfoil Dynamic Stall Control," *Journal of Aircraft*, Vol. 44, (4), 2007.

3. Khoshaljeh, M., Bae, E., and Gandhi, F., "Helicopter Performance Improvement with Variable Chord Morphing Rotors," Proceedings of the 36th European Rotorcraft Forum, Paris, France, September 2010.

4. Gandhi, F., and Hayden, F., "Design, development, and hover testing of a helicopter rotor blade chord extension morphing system," *Smart Materials and Structures*, Vol. 24, (035024), 2015, pp. 14.

5. Koratkar, N. A., and Chopra, I., "Analysis and Testing of a Froude Scaled Helicopter Rotor with Piezoelectric Bender Actuated Trailing-Edge Flaps," Vol. 8, 1997.

6. Koratkar, N. A., and Chopra, I., "Analysis and Testing of Mach-Scaled Rotor with Trailing-Edge Flaps," *AIAA Journal*, Vol. 38, (7), 2000, pp. 1113–1124.

7. Leon, O., and Gandhi, F., "Rotor Power Reduction using Multiple Spanwise Segmented, Optimally-Actuated Tailing-Edge Flaps," Proceedings of 35th European Rotorcraft Forum, Hamburg, Germany, September 2009.

8. Gandhi, F., "On Power and Actuation Requirement in Swashplateless Primary Control of Helicopters using Trailing-Edge Flaps," *The Aeronautical Journal*, Vol. 118, (1203), 2014, pp. 503.

9. Chen, P. C., and Chopra, I., "Hover Testing of Smart Rotor with Induced-Strain Actuation of Blade Twist," *AIAA Journal*, Vol. 35, (1), 1997, pp. 6–16.

10. Han, D., Pastrikakis, V., and Barakos, G., "Helicopter flight performance improvement by dynamic blade twist," *Aerospace Science and Technology*, Vol. 58, 2016, pp. 445–452.

11. Han, D., Pastrikakis, V., and Barakos, G., "Helicopter performance improvement by variable rotor speed and variable blade twist," *Aerospace Science and Technology*, Vol. 54, 2016, pp. 164–173.

12. Szodruch, J., "The Influence of Camber Variation on the Aerodynamics of Civil Transport Aircraft," 23rd Aerospace Sciences Meeting, Reno, N.V., USA, January 1985.

13. Monner, H., Hanselka, H., and Breitbach, E., "Development and Design of Flexible Fowler Flaps for an Adaptive Wing," 5th Annual Internation Symposium on Smart Structures and Materials, San Diego, CA, USA, 1998.

14. Roglin, R., Kondor, S., and Hanagud, S., "Adaptive Airfoils for Helicopter," Adaptive Structures forum, Hilton Head, SC, USA, April 1994.

15. Murugan, M., Woods, B., and Friswell, M., "Morphing Helicopter Rotor Blade with Curvilinear Fiber Composites," Proceedings of 38th European Rotorcraft Forum, Amsterdam, The Netherlands, September 2012.

16. Grohmann, B., Maucher, C., and Jänker, P., "Actuation Concepts for Morphing Helicopter Rotor Blades," 25th International Congress of the Aeronautical Sciences, Hamburg, Germany, September 2006.

17. Rauleder, J., van der Wall, B. G., Abdelmoula, A., Komp, D., Kumar, S., Ondra, V., Titurus, B., and Woods, B. K., "Aerodynamic Performance of

Morphing Blades and Rotor Systems," Proceedings of AHS International 74th Annual Forum and Technology Display, Pheonix, Arizona, USA, May 2018.

18. Amri, H., Feil, R., Hajek, M., and Weigand, M., "Possibilities and difficulties for rotorcraft using variable transmission drive trains," *CEAS Aeronautical Journal*, Vol. 7, (2), 2016, pp. 333 – 344.

19. Xie, J., Guan, N., Zhou, M., and Xie, Z., "Study on the Mechanism of the Variable-Speed Rotor Affecting Rotor Aerodynamic Performance," *Applied Sciences*, Vol. 8, (7), 2018, pp. 1030.

20. Moser, P., Barbarino, S., and Gandhi, F., "Helicopter Rotor-Blade Chord Extension Morphing Using a Centrifugally Actuated Von Mises Truss," *Journal of Aircraft*, Vol. 51, (5), 2014, pp. 1422–1431.

21. Zahoor, Y., De Breuker, R., and Voskuijl, M., "Preliminary Design of a TE Morphing Surface for Rotorcraft," AIAA Scitech 2020 Forum, Orlando, Florida, January 2020.

22. Vidyarthi, K., Beuker, M., Yin, F., Voskuijl, M., and Pavel, M. D., "HOPLITE - A Conceptual Design Environment for Helicopters Incorporating Morphing Rotor Technology," Proceedings of 44th European Rotorcraft Forum, Delft, The Netherlands, September 2018.

23. Pitt, D. M., and Peters, D. A., "Theoretical Prediction of Dynamic-Inflow Derivatives," Proceedings of 6th European Rotorcraft and Powered Lift Aircraft Forum, Bristol, England, September 1980.

24. Drela, M., and Giles, M. B., "Viscous-Inviscid Analysis of Transonic and Low Reynolds Number Airfoils," *AIAA Journal*, Vol. 25, (10), 1987, pp. 1347–1355.

Table 1: Rotor Geometrical Parameters

Characteristic	Metric	English
Radius	4.912 m	16.115 ft
Chord	0.27 m	0.885 ft
Number of blades	4	
First aerodynamic section	20% radius	
Airfoil section	NACA 23012	
Angular velocity	44.4 rad/sec	
Twist between root and tip	-8 deg (linear)	

Table 2: Flight conditions for numerical analysis

Flight Condition	Characteristic	Metric	English
Sea-Level Hover	Altitude	Sea-level	
	Velocity	0 m/s	0 ft/sec
	Flight path angle	0 deg	
Vertical Climb	Altitude	Sea-level	
	Velocity	7 m/s	23 ft/sec
	Flight path angle	90 deg	
Hover at Altitude	Altitude	2000 m	6562 ft
	Velocity	0 m/s	0 ft/sec
	Flight path angle	0 deg	

Table 3: Test Matrix for numerical analysis

Flight Condition	100% RPM	95% RPM	90% RPM
Sea-Level Hover	Active, Passive, Constant Collective	Passive	Passive
Vertical Climb at sea-level	Active, Passive	Passive	Passive
Hover at 2000 m	Active, Passive, System comparison	Passive, System comparison	Passive, System Comparison

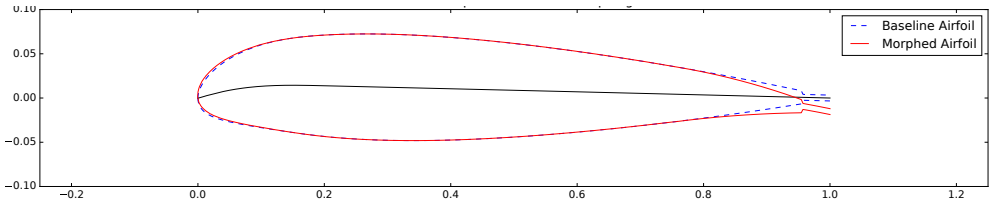

Figure 1: Morphed airfoil shape comparison with un-morphed (baseline) airfoil, for NACA 23012 airfoil.

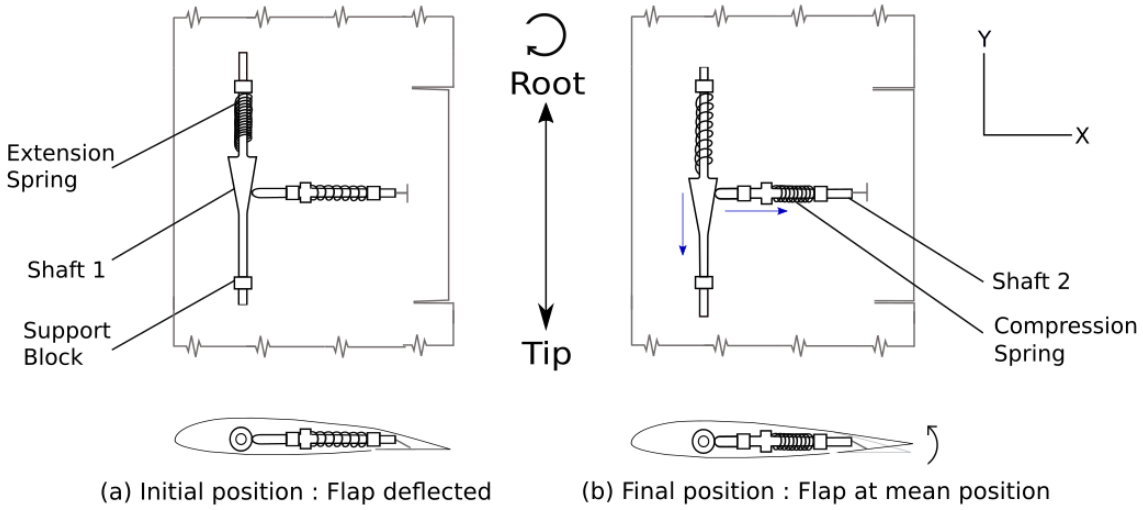

(a) Initial position : Flap deflected (b) Final position : Flap at mean position

Figure 2: Passive camber morphing actuation system concept.

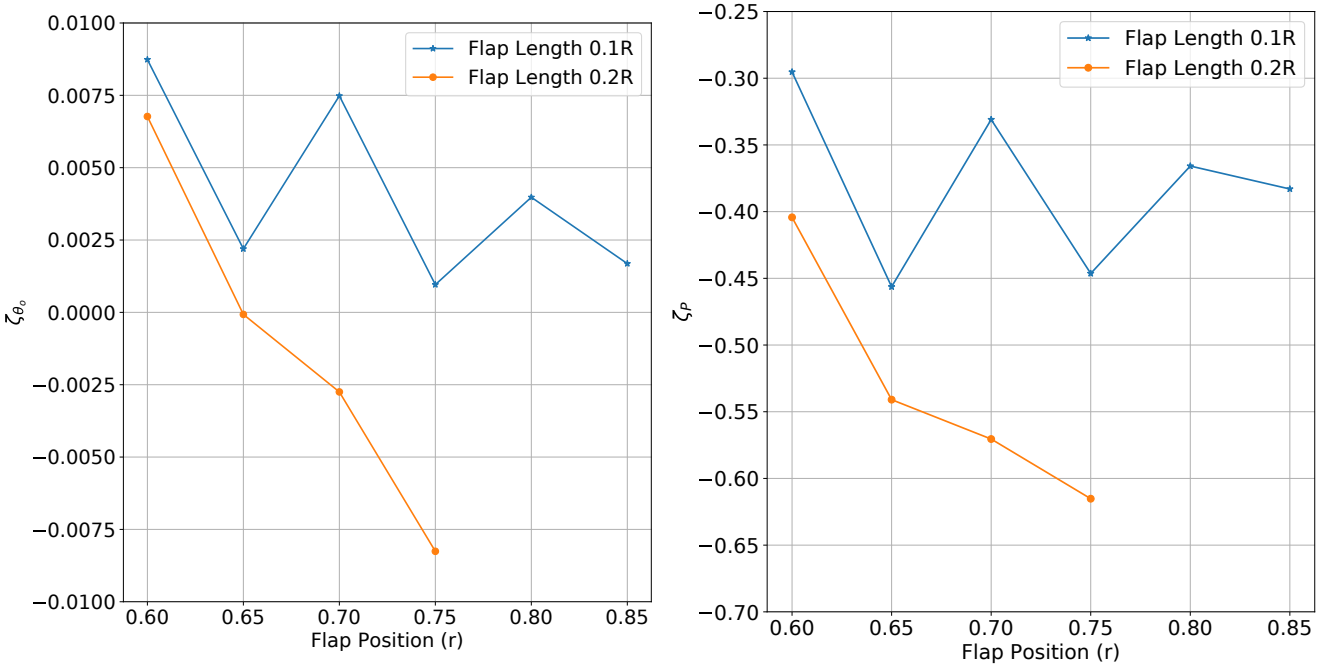

(a) Control effectiveness vs Morphing flap position

(b) Power effectiveness vs Morphing flap position

Figure 3: Camber morphing effectiveness for varying flap position

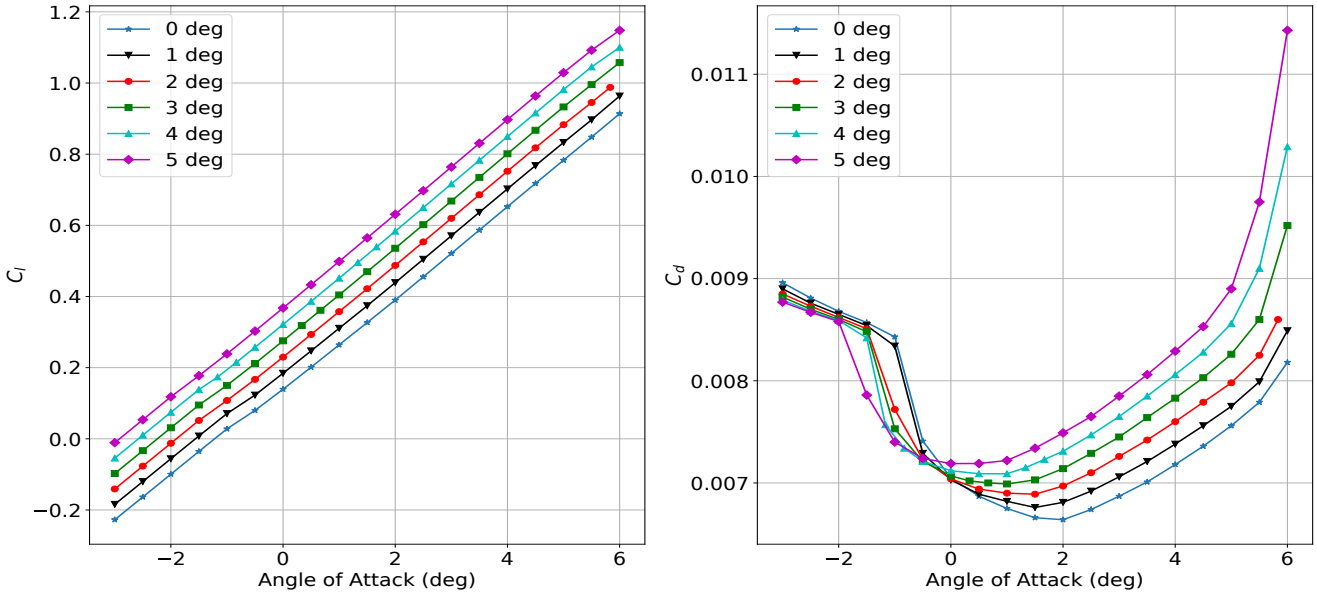

(a) Lift Coefficient vs Angle of Attack

(b) Drag Coefficient vs Angle of Attack

Figure 4: Effect of camber morphing on airfoil polars

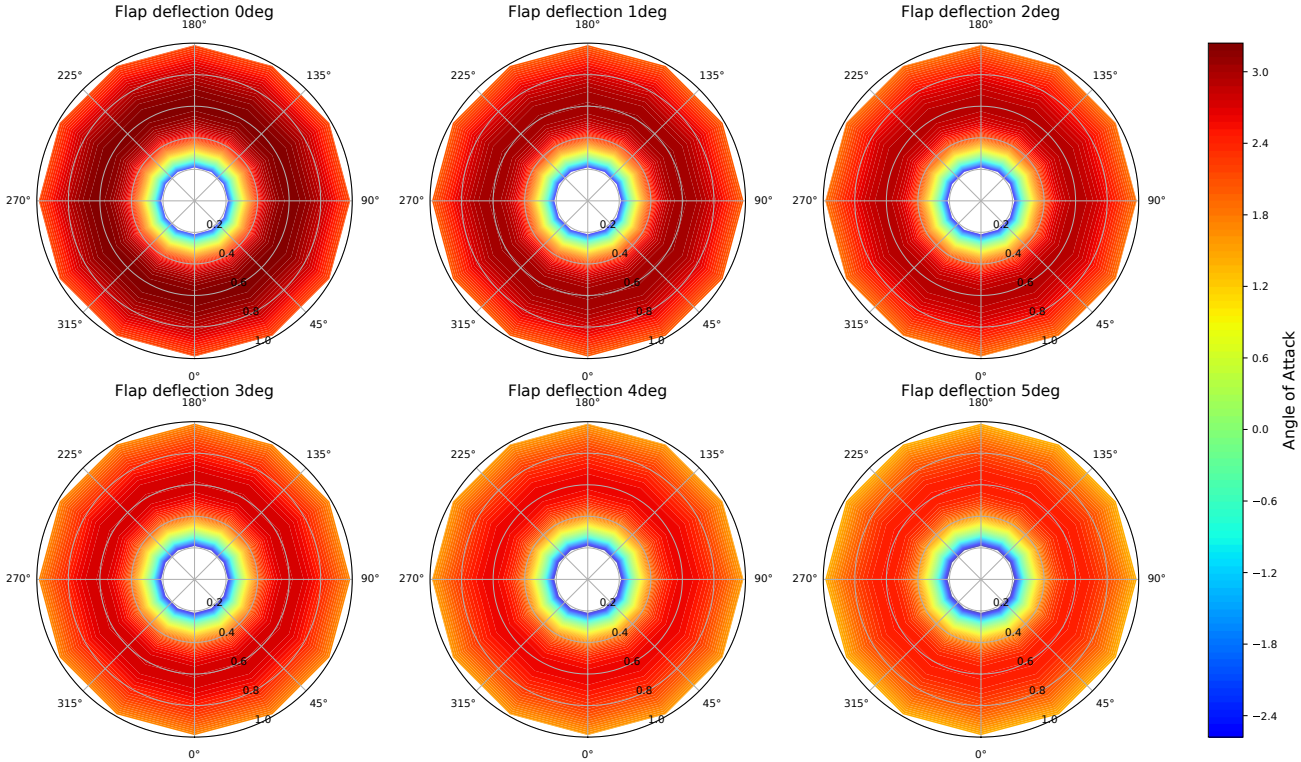

Figure 5: Variation of local section angle of attack on the rotor disk with increasing morphing flap deflection

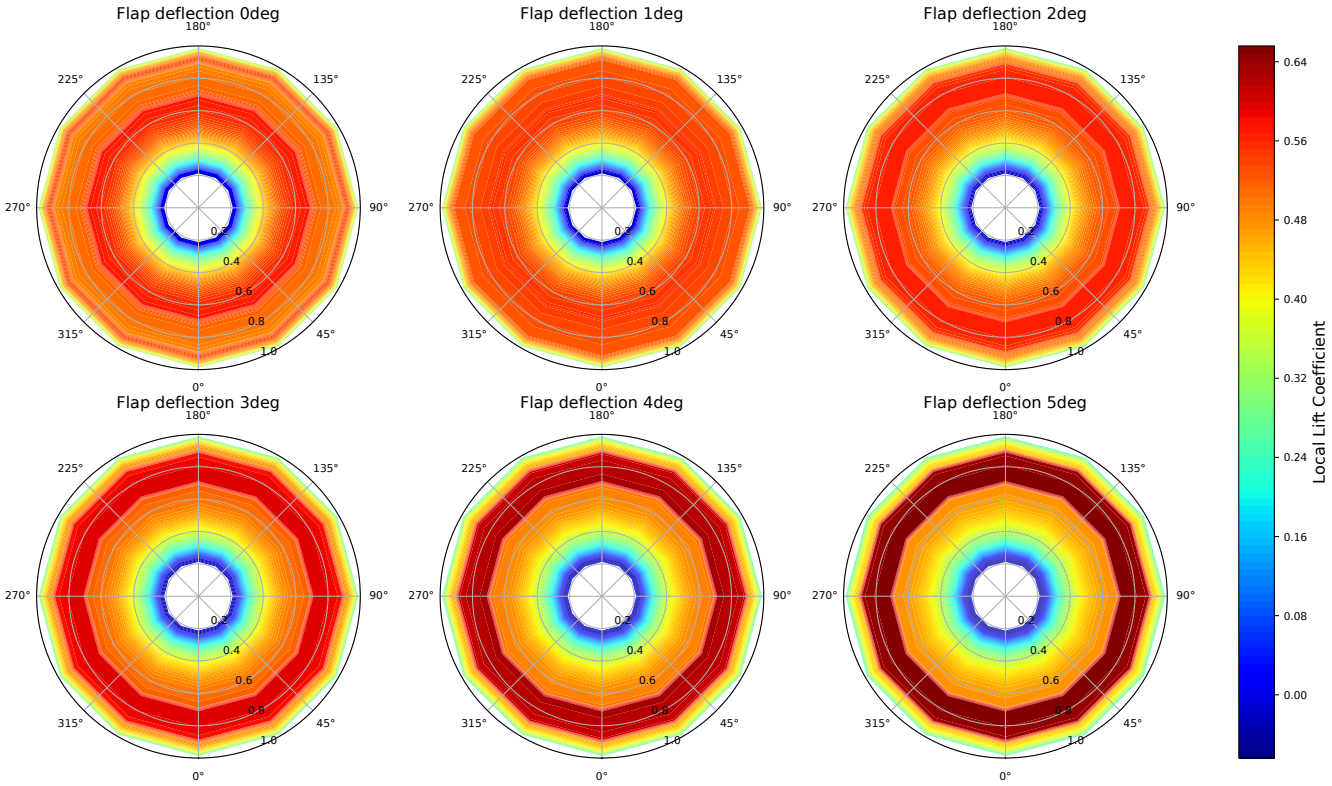

Figure 6: Variation of lift coefficient on the rotor disk with increasing morphing flap deflection

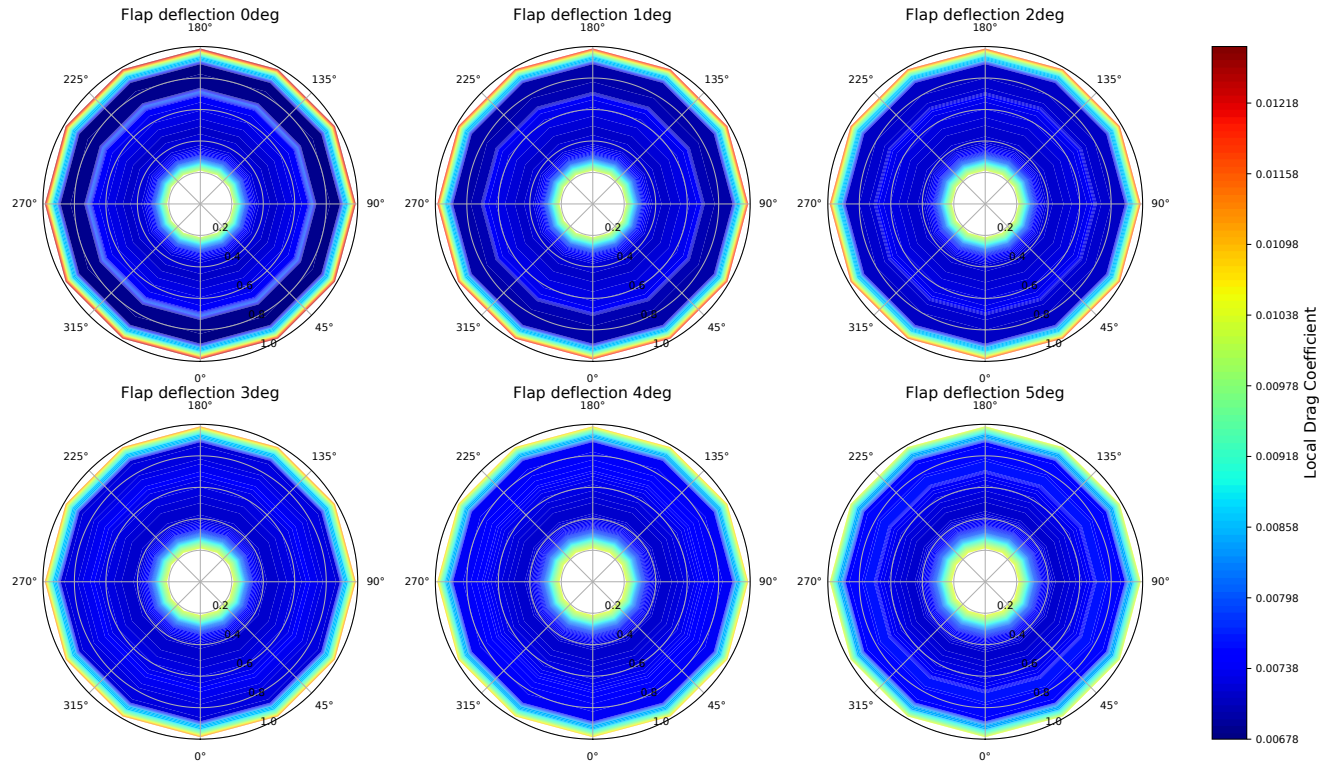

Figure 7: Variation of drag coefficient on the rotor disk with increasing morphing flap deflection

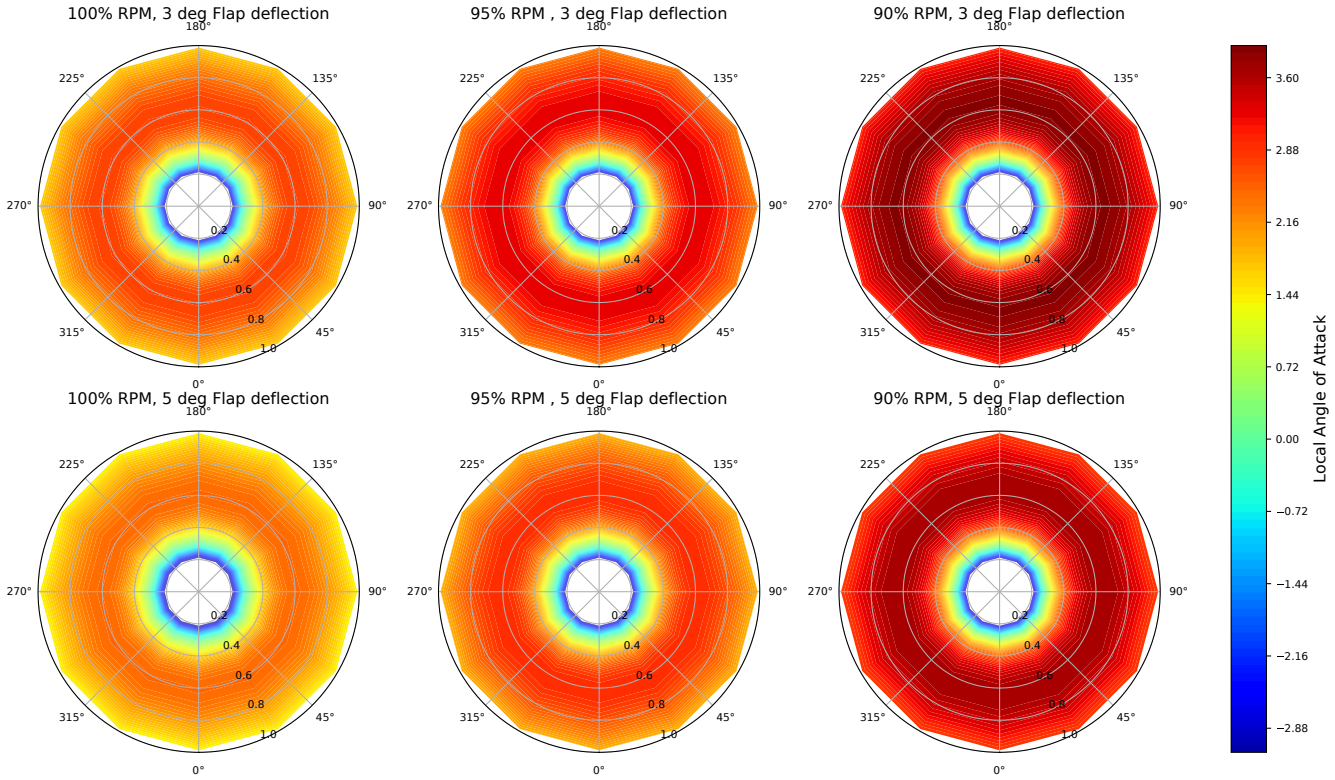

Figure 8: Variation of local angle of attack on the rotor disk with reduction of rotor RPM and flap deflections of 3 and 5 deg

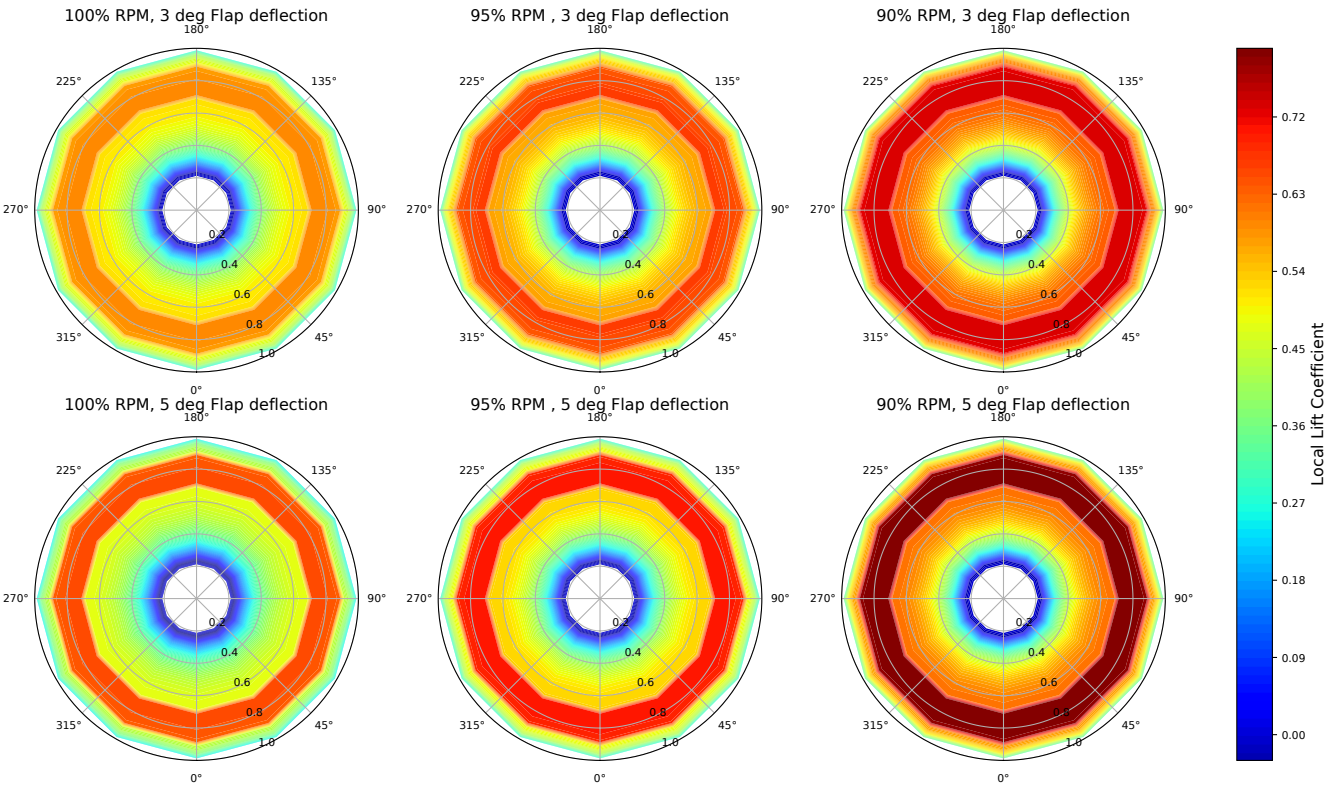

Figure 9: Variation of lift coefficient on the rotor disk with reduction of rotor RPM and flap deflections of 3 and 5 deg

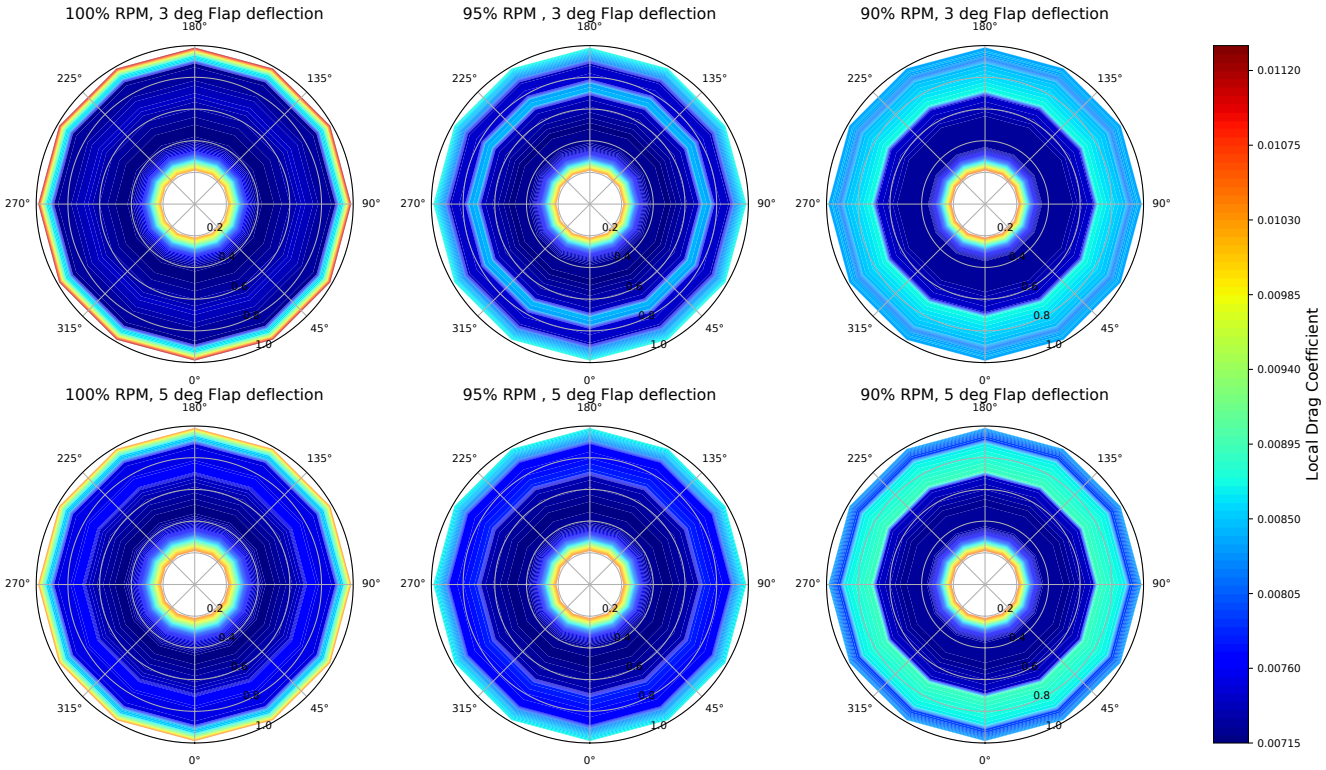

Figure 10: Variation of drag coefficient on the rotor disk with reduction of rotor RPM for and flap deflections of 3 and 5 deg

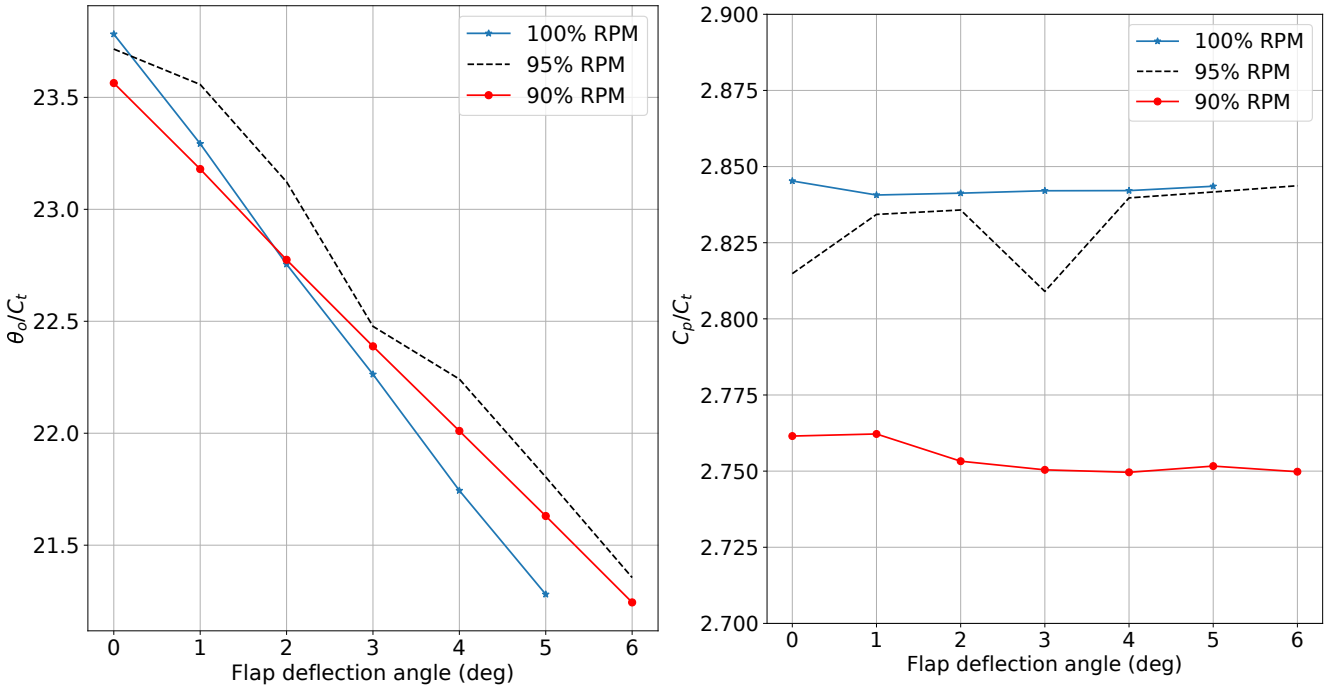

(a) Collective pitch vs flap deflection

(b) Power coefficient vs flap deflection

Figure 11: Camber morphing system performance for sea-level hover condition

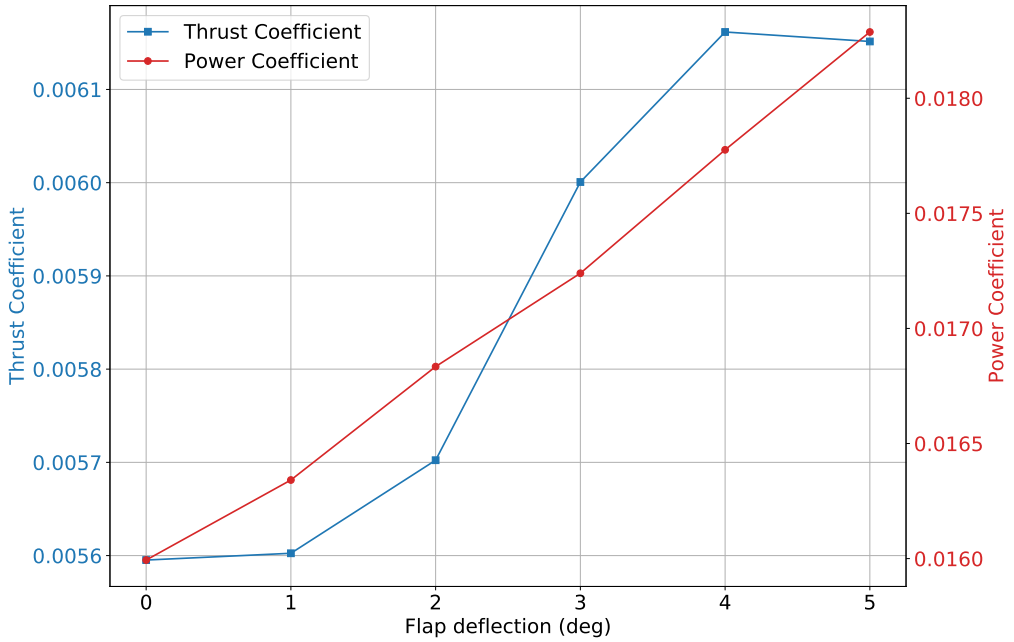

Figure 12: Variation of rotor force coefficients with increasing morphing flap deflection for fixed collective control input (7.5 deg)

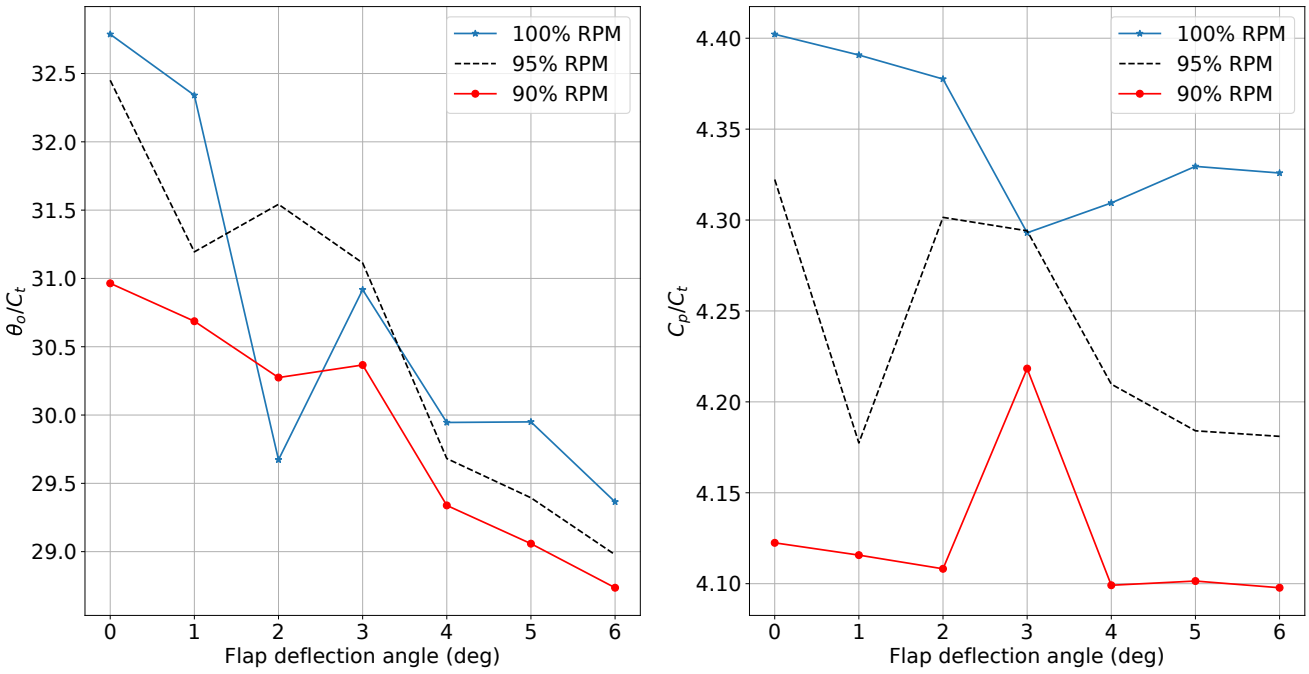

(a) Collective pitch vs flap deflection

(b) Power coefficient vs flap deflection

Figure 13: Camber morphing system performance for climb condition at sea-level

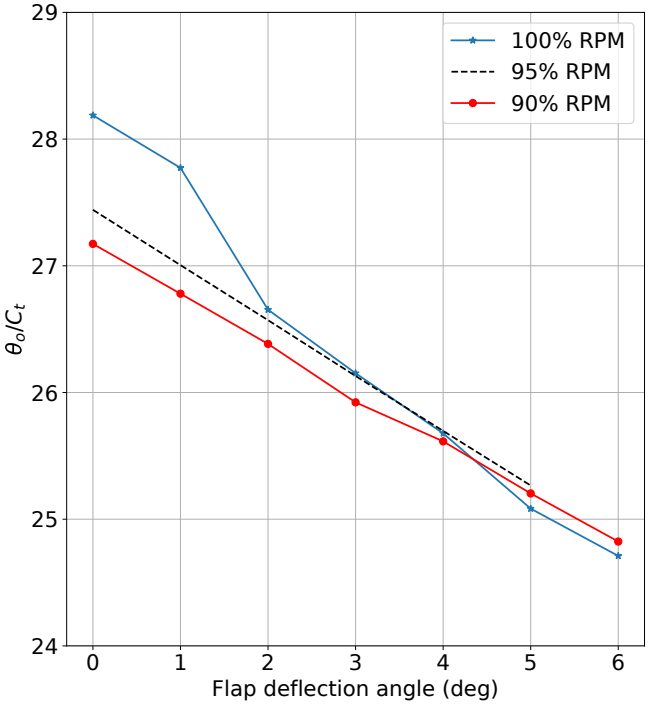

(a) Collective pitch vs flap deflection

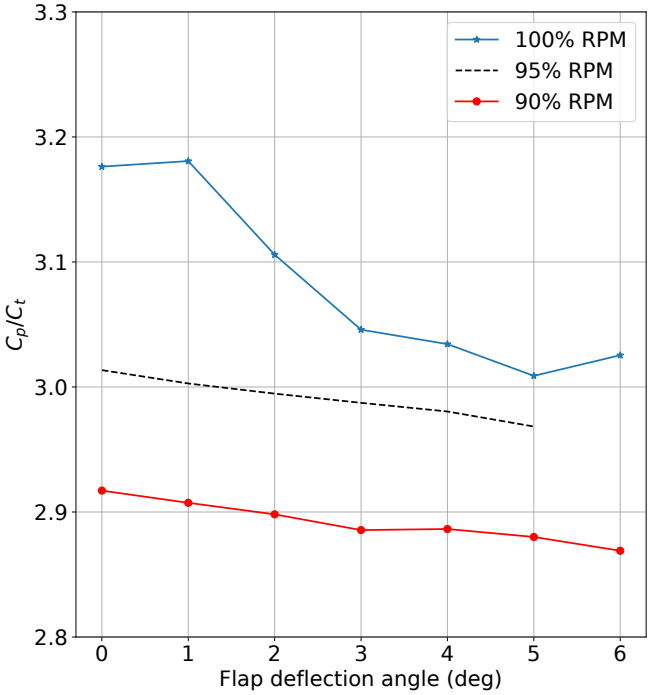

(b) Power coefficient vs flap deflection

Figure 14: Camber morphing system performance for hover condition at 2000m altitude